



**HAL**  
open science

## Partners modulate information exchange during physical interaction to adapt to task difficulty

Clémentine Colomer, Mukesh Dhamala, Gowrishankar Ganesh, Julien Lagarde

### ► To cite this version:

Clémentine Colomer, Mukesh Dhamala, Gowrishankar Ganesh, Julien Lagarde. Partners modulate information exchange during physical interaction to adapt to task difficulty. 2022. hal-03814344

**HAL Id: hal-03814344**

**<https://hal.science/hal-03814344>**

Preprint submitted on 13 Oct 2022

**HAL** is a multi-disciplinary open access archive for the deposit and dissemination of scientific research documents, whether they are published or not. The documents may come from teaching and research institutions in France or abroad, or from public or private research centers.

L'archive ouverte pluridisciplinaire **HAL**, est destinée au dépôt et à la diffusion de documents scientifiques de niveau recherche, publiés ou non, émanant des établissements d'enseignement et de recherche français ou étrangers, des laboratoires publics ou privés.

1 **Partners modulate information exchange during physical interaction to adapt to**  
2 **task difficulty**

3  
4 C. Colomer<sup>1\*</sup>, M. Dhamala<sup>2</sup>, G. Ganesh<sup>3</sup>, J. Lagarde<sup>1</sup>

5 <sup>1</sup> EuroMov Digital Health in Motion, Univ Montpellier, IMT Mines Ales,  
6 Montpellier, France

7 <sup>2</sup> Department of Physics and Astronomy, Neuroscience Institute, Georgia State  
8 University, USA

9 <sup>3</sup> Laboratoire d'Informatique, de Robotique et de Microélectronique de Montpellier  
10 (LIRMM), Univ. Montpellier, CNRS, France.

11 \*Corresponding author's email: clementine.colomer@umontpellier.fr

12

13 **Abstract**

14 The haptic sense is an important mode of communication during physical interactions,  
15 and it is known to enable humans to estimate key features of their partner's behavior.  
16 It is proposed that such estimations are based upon the exchange of information  
17 mediated by the interaction forces, resulting in role distribution and coordination  
18 between partners. In the present study, we examined whether the information  
19 exchange is functionally modified to adapt to the task, or whether it is a fixed process,  
20 leaving the adaptation to individual's behaviors. We analyzed the forces during an  
21 empirical dyadic interaction task using Granger-Geweke causality analysis, which  
22 allowed us to quantify the causal influence of each individual's forces on their  
23 partner's. We observed an increase of inter-partner influence with an increase in the  
24 difficulty of the task, demonstrating an adaptation of information flow to the task. The  
25 influence was dominated by participants in a specific role, showing a clear role  
26 division as well as task division between the dyad partners. Moreover, the influence  
27 occurred in the [2.15-7] Hz frequency band, demonstrating again its importance as a  
28 frequency band of interest during cooperation involving haptic interaction.

29 Haptic interaction – Granger-Geweke causality – Task division – Role division -  
30 Submovements

31

32 **1. Introduction**

33 Interpersonal physical interactions occur frequently in our everyday life and have  
34 been studied in the laboratory, be it to carry heavy objects (Fumery et al., 2021),  
35 dance with a partner (Sawers et al., 2017), stand-up (Sofianidis et al., 2012), or walk  
36 hand in hand with someone, it helps us coordinate and work together, but also sooth  
37 and comfort each other (Cascio et al., 2019; Gallace & Spence, 2010). Relying on  
38 both social cues (see Sailer & Leknes, 2022,) and mechanical modalities like forces  
39 amplitudes, vibration, or pressure, transmitted by somesthetic and kinesthetic  
40 receptors (see Lederman & Klatzy, 2009, for review), the haptic sense is involved in  
41 physical interactions as an important mode of communication, and it is known to  
42 enable humans to estimate features of their partner's behavior, like their movement  
43 goals (Takagi et al., 2017, 2018), their similarity (Ganesh et al., 2014), or even to

44 predict their partner's future actions (Sabu et al., 2020, Sebanz & Knoblich., 2009,  
45 Knoblich & Jordan, 2003). It is proposed that such estimations are based upon the  
46 exchange of information mediated by the interaction forces, a process sometimes  
47 dubbed as an "haptic channel" (van der Wel et al., 2011), resulting in role distribution  
48 (Chackochan et al.,2019, Curioni et al. 2019, Jarrassé et al. 2014), and coordination  
49 between partners (Sylos-Labini et al., 2018). Deciphering how the haptic channel  
50 arises and what are its specific properties is an active research topic. In an earlier  
51 study (Colomer et al., in press), we found that task related information transfer  
52 between partners in a dyad is asymmetric depending on the roles in the task, and takes  
53 place at frequencies higher than the main frequency of the movement performed to  
54 achieve the task, in the range of [2.15-7] Hz. To do so we used the Granger-Geweke  
55 causality framework, that we will introduce in the following, to analyze forces in a  
56 dyadic interaction (Geweke, 1982; Granger, 1969).

57 The distribution of the influence across frequencies may have some connections to the  
58 recurrent assumption that the control the brain exerts is parceled out in distinct  
59 frequencies, which dates back to Woodworth (1899). It has been long suggested that  
60 movements are the aggregation of submovements to form a full goal directed  
61 kinematic trajectory (Miall et al., 1993). Submovements have been previously related  
62 to an oscillatory activity in the motor cortex, phased locked with hand speed in the  
63 range of [2-5] Hz (Jerbi et al., 2007). Oscillatory components of submovements have  
64 also been identified during visual dyadic imitation and synchronization, in the range  
65 of [2-3] Hz (Noy et al. 2011; Tomassini et al., 2022).

66 Granger causality analysis uses the autoregressive modelling framework developed by  
67 Norbert Wiener (see Bressler & Seth, 2011; Granger, 1969). Granger causality is a  
68 bivariate approach, which quantifies the influence of the past of a stochastic process *A*  
69 on the present and future of another stochastic process *B*, and vice versa. This  
70 asymmetric measure provides the quantitative estimation of two directions of  
71 influence. The underlying rationale is as follows: If the predictability of the  
72 independent system *B* is improved by the incorporation of information from  
73 independent system *A*, then it can be concluded that *A* influences *B*. In our previous  
74 study, we analyzed the time series of forces produced by the two partners during  
75 physical interaction. We used the Granger-Geweke causality (GGC) (Geweke, 1982)  
76 for this, which allows deriving Granger causality in the frequency domain. Granger-  
77 Geweke causality affords a fine grain decomposition of the direction of exchange  
78 between partners as a function of frequency, which departs from previous attempts to  
79 identify asymmetry in haptic coupling (Huys et al., 2018). The method provided us  
80 with "Granger causality values" that we renamed "influence", and was shown to be a  
81 reliable signature of information exchange between them (Colomer et al., 2022).

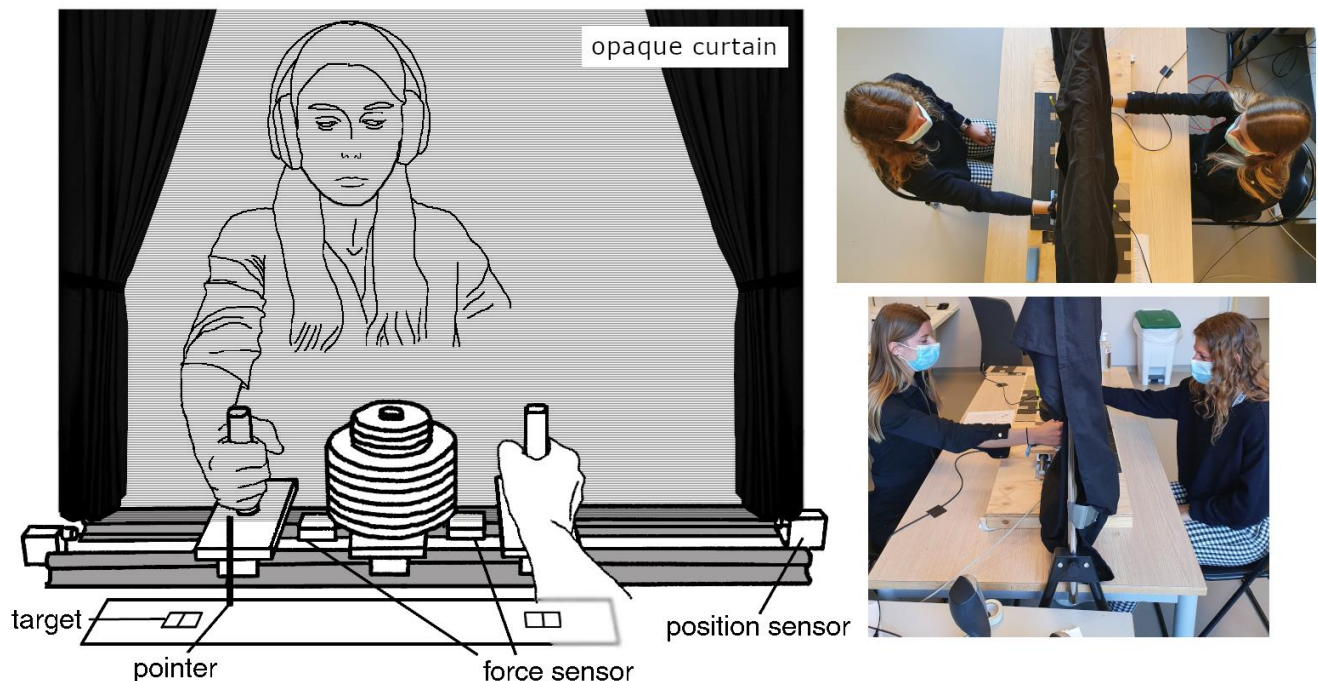
82 Following our previous study (Colomer et al., In press), we used a task imposing a  
83 division of labor: Both partners were moving a unique mobile slider, to do so one  
84 partner had to synch with beats sequence while the other had to point at visual targets  
85 (See Fig.1 and Experimental set-up). In the present study, we examined whether the  
86 information exchange is a fixed process which depends only on the general leader/  
87 follower roles due to the labor division between partners, or if it is instead  
88 functionally modified to adapt to the difficulty of the task. We made the hypothesis

89 that a more ‘difficult’ task would result in a higher quantity of information exchanged,  
90 and / or a change in the main direction of the influence. The difficulty of the task was  
91 modulated according to Fitts law by reducing the width of visual targets (Fitts, 1954).

92

## 93 2. Materials and Methods

94 Our study was carried out according to the principles expressed in the Declaration of  
95 Helsinki, and were approved by the EuroMov ethical committee (EuroMov IRB  
96 #1912A, University of Montpellier). All participants provided written informed  
97 consent to participate in the study. In addition, all participants gave informed consent  
98 for publication of identifying images (i.e., Fig.1) in an online publication.



100 **Fig. 1) Experimental setup.** Our setup consists of a rigid passive slider manipandum with  
101 two handles. The slider slides on two rails on roller bearings to reduce friction. A rack in the  
102 center of the manipandum allows us to load the slider. Position encoders and two 1-dof  
103 force sensors (near each handle) allows us to record the participant movements and forces.  
104 Participants performed in dyads in our task. They sat on opposite sides of the table and held  
105 one handle with their right hand and made reciprocal aiming movement to left and right  
106 targets (visible to one participant only) while synchronizing as accurately as possible with a  
107 metronome provided to them using headphones (one participant only). A curtain along the  
108 axis of the slider prevented the participants from seeing their partner and their handle. The  
109 participants were provided with targets towards which they had to perform a reciprocal  
110 pointing task with a vertical pointer fixed on the device; they had to aim inside the target box,  
111 the middle line served as visual help for their positioning.

112

### 113 2.1. Experimental Design

114 Our experiment required participant dyads to move a one-degree of freedom passive  
115 mobile slider manipandum with two handles, one for each participant (see Fig. 1).

116 Each handle was equipped with a force sensor allowing us to evaluate the force applied  
117 by each participant. A curtain along the axis of the manipulandum prevented the  
118 participants from seeing their partner and the partner's handle. The task the participants  
119 had to perform was a cooperative task where both members of the dyad had to move a  
120 mobile device (Fig. 1) based on two cues: visual targets and metronome beats. We  
121 recorded (at 500 Hz) the mobile slider's position using 2 Linear Position Transducer,  
122 and each participant's applied force with 2 compression and tension load cells. We used  
123 2 A/D cards (NI USB 6229 16-bit Digital Acquisition Board) for force and position,  
124 and custom Matlab® programs. The auditory metronome was displayed using a custom  
125 Matlab® program and PC computer sound card (Intel®), duration = 80ms, sinewave,  
126 tone = 500 Hz. Beat events were recorded along all sensors, using an A/D card (NI USB  
127 6002 16-bit Digital Acquisition Board).

128

129 20 participants (10 dyads, aged between 18 and 40, 11 females) participated in the  
130 experiment, in which they had to move a manipulandum weighting 16.5kg. Each  
131 participant was weighted at the end of the experiment and the de Leva table (de Leva,  
132 1996) used to calculate their hand and forearm's mass. Expert musicians and dancers  
133 (10 years of regular practice) were excluded from this study, as well as people  
134 practicing rhythmic or interpersonal coordinative sports.

135 Inspired by a study of timing processes in single person (Craig & Lee, 2005), our task  
136 required the dyads to repeatedly move the mobile slider to reach two targets on the  
137 table located on opposite sides from the central position of the manipulandum, while  
138 synchronizing their movements with an audio metronome. In order to increase  
139 information exchange between participants, we divided the feedbacks available for  
140 each participant. In each dyad the 'Synch Participant' was given the metronome to be  
141 followed (using earphones) but was not provided with the target positions that defined  
142 the movement range. The other partner, the 'Target Participant', was provided with  
143 the target information, but not the metronome which defined the movement timings to  
144 be maintained. Both participants were instructed about the arrangement. They knew  
145 that they were required to make repeated movements to targets while following a  
146 metronome as best as possible while cooperating, and knew that each participant  
147 received only one feedback.

148 The participants worked in two conditions. The target width and rate of the metronome  
149 were different between the 2 conditions. In the 'small target condition', the target size  
150 was 1 cm on both ends of the pointing task. In the 'large target condition' the target  
151 width was set as 2 cm. The distance between the target's centers was fixed at 23cm.  
152 Before each session we asked the Target Participants to perform solo trials for each  
153 target condition, with the instruction to move to the targets at the maximal speed they  
154 could reach without making mistakes. Metronome beat rates for each target condition  
155 then corresponded to the mean of this preferential frequency. For all dyads, the  
156 preferred time period was faster in the large target condition ( $0,8\pm 0,2$  seconds mean)  
157 than in the small target condition ( $0,9\pm 0,2$  seconds mean).

158 One trial lasted 20 beats (between ~12 and ~23 seconds depending on the target width  
159 condition) and each dyad had to do 9 trials per condition. Overall each dyad performed  
160 18 trials where conditions were randomized.

161 At the beginning of each trial a random interval of a few seconds of silence was inserted  
162 before the beat metronome started, so the participants would not use the experimenter  
163 start instruction as first temporal cue.

164

## 165 **2.2 Task difficulty**

166 To modulate our task difficulty, we looked at Fitts' law (Fitts, 1954) and chose to use  
167 2 different target sizes for the participants to reach, with the smaller one as our more  
168 difficult condition. Even if the difficulty change was in the spatial domain, that is Target  
169 Participants' task, Sync Participants will need to increase their attention as the frame in  
170 which they have to synchronize the mobile's change of direction will also reduce with  
171 the target's width.

172 To ensure that this condition was indeed more difficult we observed our participants  
173 movement speed and error indices during both conditions using one-sample t-tests. We  
174 made the hypothesis that the more difficult condition would have slower movements  
175 and higher error scores.

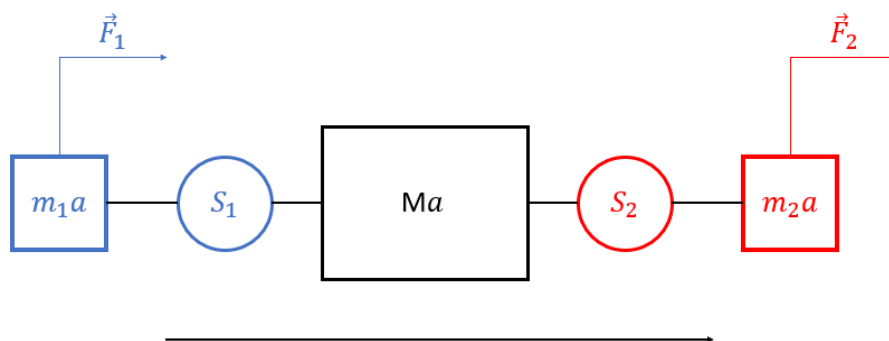
176

## 177 **2.3 Data processing**

178 Participant Forces and the mobile slider's position were both measured in Volts.  
179 Positions were subsequently converted to centimeter and forces to Newtons, and both  
180 were low pass filtered (Butterworth filter, dual pass, cut off frequency 10 Hz).

181 From the time series of the beats, we detected each onset using the function  
182 *findpeaks.m* in Matlab®. To measure the frequency content of each participant's force  
183 time series, we used a local minima and maxima detection method, using the function  
184 *findpeaks.m* from Matlab®, to get the distribution of periods. This was then converted  
185 to frequency in Hz.

186 The participant forces were estimated from the sensors according to the model  
187 presented in Figure 2.



188

189 **Fig. 2) Model used to estimate forces from the sensors.** Where  $\overline{m_1 a}$  and  $\overline{m_2 a}$  represent the  
 190 mass (hand + forearm) multiplied by the acceleration,  $\overline{Ma}$  the central mass of the mobile  
 191 slider multiplied by acceleration,  $\overline{S_1}$  and  $\overline{S_2}$  are the sensor measured force, and  $\overline{F_1}$  and  $\overline{F_2}$  the  
 192 force applied by the two participants respectively. We consider the effects of friction as being  
 193 negligible.

194 In Figure 2, where  $\overline{m_1 a}$  and  $\overline{m_2 a}$  represent the mass (hand + forearm) multiplied by  
 195 the acceleration,  $\overline{Ma}$  the central mass of the mobile multiplied by acceleration,  $\overline{S_1}$  and  
 196  $\overline{S_2}$  are the sensor measured force, and  $\overline{F_1}$  and  $\overline{F_2}$  the force applied by the two  
 197 participants respectively. We consider the effects of friction as being negligible.

198 Taking a movement toward the right as positive, we consider the free body diagram of  
 199 mass  $m_2$  to get:

$$200 \quad \overline{F_2} = \overline{m_2 a} + \overline{S_2} \quad (1)$$

201 Considering the free body diagram of mass  $M$ :

$$202 \quad \overline{S_2} - \overline{S_1} = \overline{Ma} \quad (2)$$

203 And considering the free body diagram of mass  $m_1$  we get:

$$204 \quad \overline{F_1} = \overline{m_1 a} - \overline{S_1} \quad (3)$$

205

206 The mass  $M$  (which was fixed in each experiment) is known, as well as the hand +  
 207 forearm mass of each participant ( $m_1$  and  $m_2$ ) were estimated for each dyad by  
 208 weighing each participant and using the de Leva table (de Leva, 1996). Substituting  
 209 for  $a$  from (2) in (1) and (3), we can calculate the force applied by each participant by  
 210 considering the directions of movements appropriately at any instance.

211

## 212 **2.4 Performance indices**

213 The Position Error (PE) was calculated using the difference between the position at  
 214 which our subjects changed direction and the edge of the target they had to reach. The  
 215 result was expressed in centimeter. A change of direction occurring inside a target box  
 216 was counted as an error of 0. The Synchronization Error (SE) was calculated as the  
 217 difference between each period of movement between two targets and the period of the  
 218 metronome for that trial. The Synchronization Error was then expressed in % of the  
 219 metronome's period.

220 We calculated the mean value and variance of errors across the 20 beats of each trial.  
 221 The average of these values across trials was used to estimate overall mean and variable  
 222 errors for each dyad per condition. In full generality, for steady behaviour, the  
 223 variability estimated by variance or standard deviation is indicative of the (asymptotic)  
 224 stability against intrinsic continuous stochastic perturbations (Kelso, 1995).

225

## 226 **2.5 Granger-Geweke causality spectral estimation**

227 Granger-Geweke causality (GGC) was estimated by using the parametric method (Ding  
 228 et al, 2006) from the forces' times series. The BSmart toolbox for the software Matlab®

229 was used, specifically the functions designed for bivariate analysis by Cui et al., 2008.  
 230 Prior to the Granger-Geweke estimation we down-sampled the forces time series to 25  
 231 Hz to address our frequency range of interest (0.1 to 10 Hz), approximating the higher  
 232 bound as the Nyquist frequency of our down sampled signals. For each trial and each  
 233 dyad, the force time series were segmented in 3 consecutive time windows of equal  
 234 durations, providing 27 data epochs for each dyad, which were fed into the GGC  
 235 analysis. This analysis method estimated the influence in the frequency domain from A  
 236 to B and from B to A.

237 According to Geweke (Geweke, 1982), the Granger causality spectrum from  $x_{Bt}$  to  $x_{At}$   
 238 is computed as follow:

$$239 \quad I_{B \rightarrow A}(f) = -\ln\left(1 - \frac{(\Sigma_{BB} - \frac{\Sigma_{AB}^B}{\Sigma_{AA}})|H_{AB}(f)|^2}{S_{AA}(f)}\right) \quad (4)$$

240 where  $\Sigma_{BB}$ ,  $\Sigma_{AB}^B$  and  $\Sigma_{AA}$  are elements of the covariance matrix  $\Sigma$ .  $S_{AA}(f)$  is the power  
 241 spectrum of channel A at frequency  $f$  and  $H(f)$  is the transfer function of the system  
 242 (see Appendix in Brovelli et al., 2004; Ding, et al., 2006; Dhamala, et al., 2008;  
 243 Dhamala, et al., 2018).

244

## 245 **2.6 Frequency bands for GGC**

246 Frequency bands of interest were defined in a previous study (Colomer et al., 2022), in  
 247 which we had used the same experimental setup and division of roles between  
 248 participants. In this previous study we demonstrated the existence of two time scales on  
 249 our frequency analysis: A lower frequency band including the repetitive motion of our  
 250 task, and a higher frequency band that encompasses the higher frequencies of  
 251 intermittent movements, as mentioned in the submovements literature.

252 More practically, frequency bands of interest were defined after the observation that the  
 253 majority of our dyads had two peaks in the Granger causality analysis, one at low  
 254 frequency range, and a second at higher frequency range. To define two frequency  
 255 bands of our interest, we first observed that the majority of our dyads had two peaks in  
 256 the Granger values. We located the first peak for every participant, and calculated the  
 257 mean and standard deviation across participants. The mean+3\*STD across participants  
 258 was calculated as 2.15 Hz. The first frequency band was thus set between 0.1 Hz and  
 259 2.15 Hz. Next, we considered the GGC values for the Synch Participants and noted that  
 260 the mean +3\*STD GGC value went below the bootstrap value at 7 Hz. The second  
 261 frequency band was thus set between 2.15 Hz and 7 Hz. A bootstrap vector (99<sup>th</sup>  
 262 percentiles of null distribution using a bivariate permutation among dyads) was used to  
 263 identify the baseline Granger values that were independent of interaction between  
 264 participants (see Colomer et al., 2022).

265 To quantify the Granger causality within each band we integrated the GGC values over  
 266 frequency in each direction of exchange using a trapezoidal numerical integration. It is  
 267 noteworthy that the integral of GGC in the frequency domain is equivalent under  
 268 general conditions to the Granger causality in the time domain (Ding et al., 2006;  
 269 Geweke, 1982).

270 Next, for each condition we calculated the difference of this integrated GGC between  
271 participants in a dyad, a variable we labelled the  $\Delta$  influence, for each of the two  
272 frequency bands. We used a two-sample t-test to look at differences in both conditions  
273 in the [2.15-7] Hz frequency band and analyzed the integral GGC values, which we  
274 compared between small and large target conditions (Fig.7) using a Wilcoxon signed  
275 rank test.

276 We also looked at the overall influence of each role in both conditions and frequency  
277 range using a Three-Way Mixed effect ANOVA. This method of analysis was chosen  
278 for we had both within-subject factors (2 Target sizes and 2 Frequency bands) and  
279 between subject factor separating our participants in 2 distinct groups (Roles). We used  
280 a Bonferroni correction on all post-hoc tests (see Supplementary figures for tables).

281

## 282 **2.7 Main statistical analysis**

283 We used a Shapiro Wilk Test to assess the normality of our data before executing any  
284 further statistical analysis, and two sampled t-test or Wilcoxon signed rank test were  
285 used accordingly.

286 To analyze the difference between the applied forces in each condition, we performed  
287 a Wilcoxon signed rank test on the mean of our forces put in absolute value, across  
288 dyads and conditions (Fig. 4A). We also analyzed the change in mean force for each  
289 role between conditions using one-sample t-tests (Fig. 4B).

290 Analyzing the frequency content of the forces, estimated from the periods obtained  
291 from local minima and maxima, we used an Empirical cumulative distribution  
292 function (ECDN) two-sample test statistic calculating the EMD distance between the  
293 distributions, and testing it against 1000 distributions obtained after random  
294 permutations (Dowd, 2020; Ramdas et al., 2017).

295 To measure the correlation between the mean force frequency and the movement time  
296 period for each participant, in each condition and for each trial, we used a Pearson  
297 correlation. We also used a Pearson correlation to measure the correlation between the  
298 difference of integral of GGC values over frequency (the  $\Delta$  influence) and the  
299 performance indices in both conditions.

300

## 301 **3. Results**

### 302 *Movement and difficulty*

303 We used our performance indices to assess the difficulty of our two conditions, with  
304 the belief that a harder task would lead to more mistakes.

305 Overall, we found significantly higher mean Synchronization Error and mean Position  
306 Error in the small target condition (SEm, T(9)=2.5, p<0.03 ; PEm, T(9)=5.8, p<0.001,  
307 one-sample t-test) than in the large target condition. No significant difference was  
308 found in the standard deviation of the Synchronization Error between conditions, but  
309 we did observe significantly higher standard deviation of Position Error in small

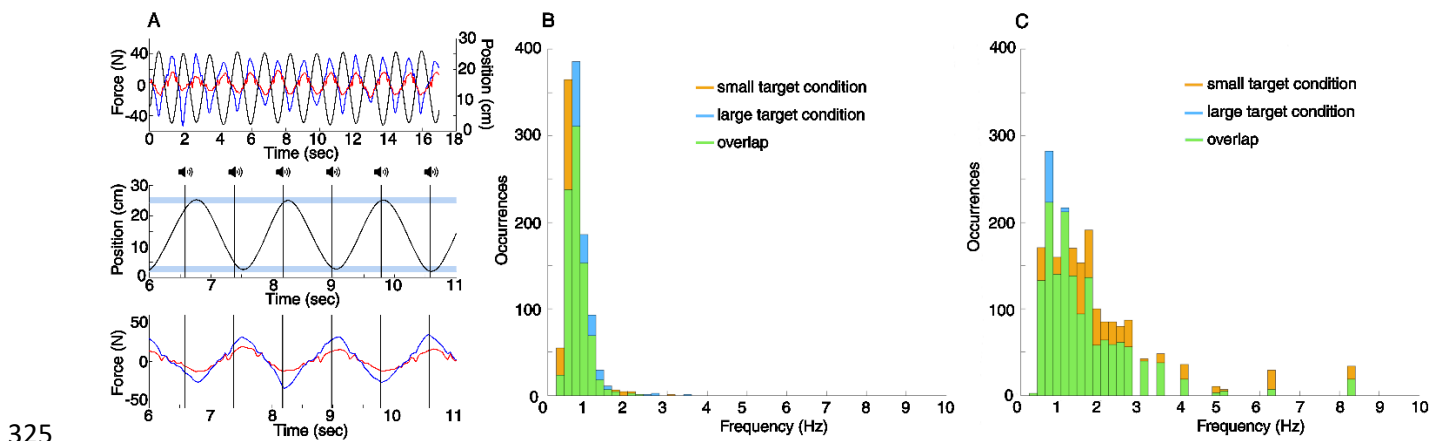
310 target condition (PEsd,  $T(9)=5.6$ ,  $p<0.001$ , one-sample t-test) compared to large target  
311 condition.

312 We found that our participants adopted significantly faster movement time period in  
313 the large target condition than in the small target condition ( $T(9)=4.6$ ,  $p<0.001$ , one-  
314 sample t-test). The mean movement time period across trials was faster in the large  
315 target condition for all dyads except one, and the mean movement time period across  
316 dyads was of 1.59 seconds for the large target condition, and 1.77 seconds for the  
317 small one.

318

### 319 *Participant forces*

320 Fig. 3 shows an example movement and recorded forces from a representative dyad in  
321 one condition. The forces' sign represented the direction at which participant applied  
322 their force (see Methods). We calculated that both participants applied forces in the  
323 same direction 70% of the time through our experiment. Absolute values were used  
324 for the rest of the results.



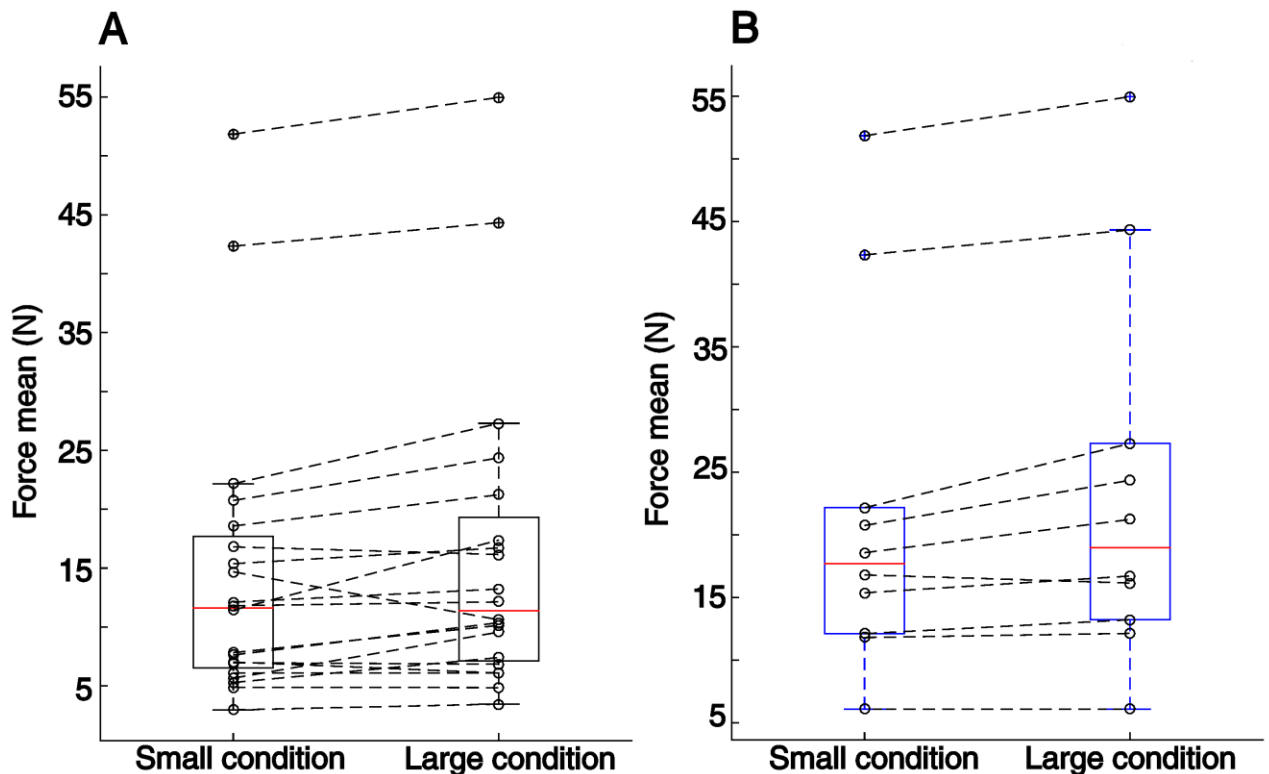
325

326 **Fig. 3) Forces time series and task behavior in a representative trial, and histograms of**  
327 **frequency content of the participant's forces' time series in each condition. A)** Example  
328 of recorded displacement of the slider (top and middle) and forces (top and bottom) from a  
329 representative dyad in small target condition. Temporal cues heard by the Synch Participant  
330 are represented as vertical black lines, and target area as horizontal pale bands. Participants  
331 were required to synchronize their change of direction with the metronome, while aiming at  
332 each target as accurately as possible. **B)** Histogram of frequency content of the Target  
333 Participants' forces' time series in small target condition (orange) and large target condition  
334 (blue). An empirical cumulative distribution function (ECDF) two-sample test was used to  
335 confirm the difference between the two distributions ( $p<0.009$ ,  $D=0.022$ ) **C)** Histogram of  
336 frequency content of the Synch Participants' forces' time series in small target condition  
337 (orange) and large target condition (blue). We confirmed the difference between the two  
338 distributions by an ECDF two-sample test ( $p<0.012$ ,  $D=0.026$ ).

339

340 The mean force by each participant across the 9 trials was significantly higher in the  
341 large target condition than in the small target condition ( $W=37$ ,  $p<0.01$ , Wilcoxon  
342 signed rank test, Fig. 4A). When examined, we found that the Synch Participant's

343 mean force did not significantly change between conditions ( $T(9)=1.4$ ,  $p<0.2$ , one-  
 344 sample t-test) but the Target Participant's did ( $T(9)=3.3$ ,  $p<0.01$ , one-sample t-test,  
 345 Fig. 4B), with smaller force mean in the small target condition compared to the large  
 346 target condition. No significant correlation was found between mean force and  
 347 influence.



348 **Fig. 4) Box plot of the force mean for each participant, as estimated from our force**  
 349 **sensors, for each condition. A)** Box plot of the total force mean for each participant (both  
 350 roles) for each condition. The total force mean was significantly more in the large target  
 351 condition compared to the small target condition ( $W=37$ ,  $p<0.01$ , Wilcoxon signed rank test).  
 352 **B)** Box plot of the force mean for each Target Participant for each condition. The total force  
 353 mean was significantly less in the small target condition compared to the large target  
 354 condition ( $T(9)=3.3$ ,  $p<0.01$ , one-sample t-test).  
 355

356 We also investigated the differences in frequency content of our participant's forces  
 357 between the small target condition and the large target condition. Using an Empirical  
 358 cumulative distribution function two-sample testing (ECDF, see Methods for more  
 359 precisions) we've found a difference between the distribution of all participants'  
 360 forces in small target condition and the distribution of all participant's forces in large  
 361 target condition ( $p<0.008$ ,  $d=0.021$ ). To better understand this difference we looked  
 362 more precisely at the frequency content histograms of each role's (Target/Synch  
 363 Participants) forces in both conditions. We've found a difference of distributions for  
 364 both roles between small and large target conditions (Target Participants,  $p<0.009$ ,  
 365  $d=0.022$ , Fig. 3B; Synch Participants,  $p<0.012$ ,  $d=0.026$ , Fig. 3C).

366 We hypothesized that this difference in forces frequency content's distribution  
 367 between conditions could be attributed to the difference in movement time period  
 368 between conditions, which was inherent to the task. We therefore analyzed the

369 correlation between the mean force frequency and the movement time period across  
370 the participants. We found a significant correlation for the Target Participants  
371 ( $p < 0.001$ , R value = 0.53, Pearson correlation) across conditions and trials, and the  
372 movement time was observed to increase force occurrences at low frequencies. We  
373 did not however find a correlation between the mean force frequency of the Synch  
374 Participants mean force frequency and movement time period ( $p < 0.32$ , R value =  
375 0.08, Pearson correlation).

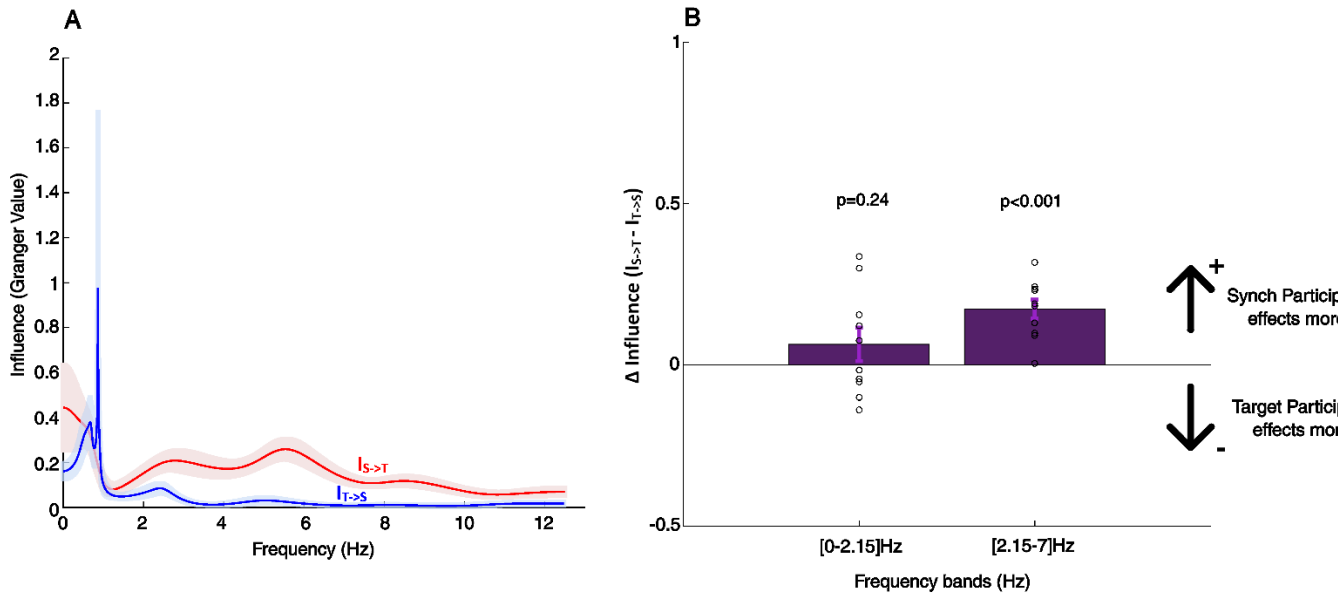
376

### 377 *Influence on partner*

378 For each condition we analyzed the forces collected in the nine trials using GGC  
379 analyses to isolate patterns that were consistent (see Methods for details). Fig. 5A  
380 shows the ‘GGC values’, which provide a quantification over each frequency of the  
381 Synch Participants’ forces’ influence on the forces produced by the Target  
382 Participants ( $I_{S \rightarrow T}$ , red trace), and vice versa ( $I_{T \rightarrow S}$ , blue trace).

383 As already stated above, we chose the same frequency bands of interest as in our  
384 previous study (Colomer et al., in press), the [0-2.15] Hz and [2.15-7] Hz frequency  
385 bands (see Methods for more details). Within these bands we calculated the  
386 differences between the integral of GGC values  $I_{S \rightarrow T}$  and  $I_{T \rightarrow S}$  for each condition (Fig.  
387 5B and Fig. 6B).

388 Our task being repetitive by nature, most of the participant force was generated at the  
389 end points of the back-and-forth motion, in order to decelerate the mobile while  
390 approaching one target and then accelerating in the opposite direction toward the next  
391 target. In both conditions the inter-personal influence ( $I_{S \rightarrow T}$  and/or  $I_{T \rightarrow S}$ ) was not  
392 significantly different in the [0-2.15] Hz band (large target  $T(18) = 1.22$ ,  $p = 0.24$ , two-  
393 sample t-test, Fig. 5B ; small target  $T(18) = 1.10$ ,  $p > 0.28$ , two-sample t-test, Fig. 6B),  
394 which corresponds to the main movement frequencies. On the other hand, we  
395 observed that  $I_{S \rightarrow T}$  was significantly larger than  $I_{T \rightarrow S}$  in the [2.15-7.0] Hz range, in  
396 both conditions (large target  $T(18) = 5.88$ ,  $p < 0.001$ , two-sample t-test, Fig. 5B ; small  
397 target  $T(18) = 5.89$ ,  $p < 0.001$ , two-sample t-test, Fig. 6B).

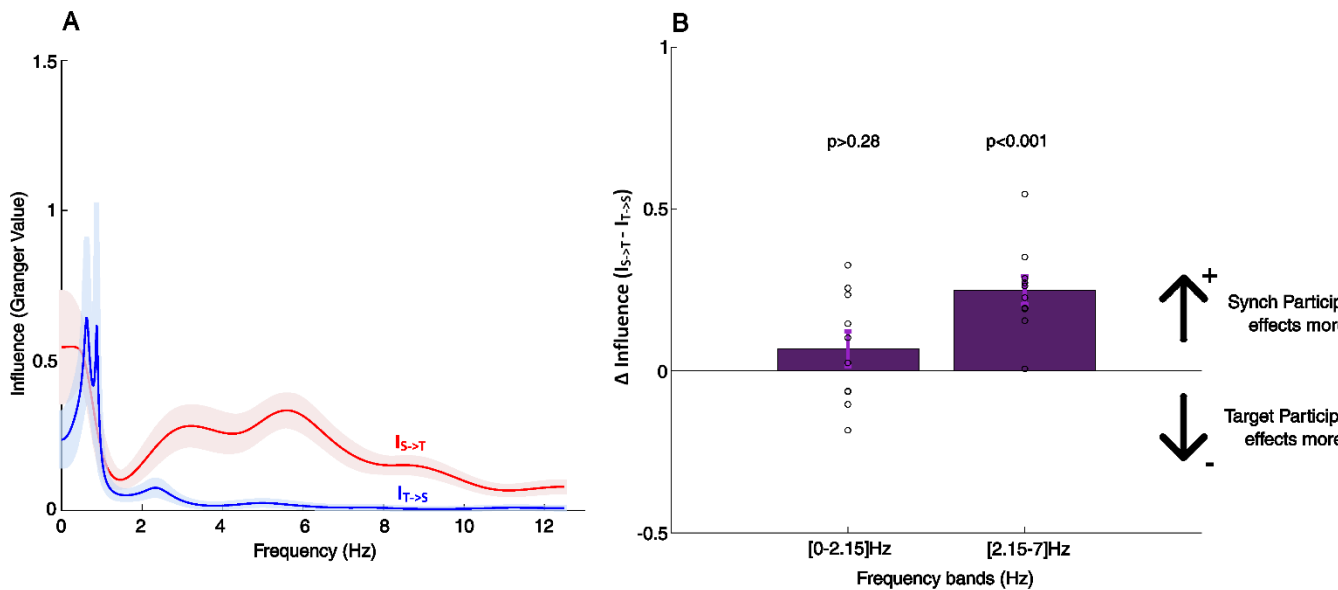


398

399 **Fig. 5) Granger-Geweke causality (GGC) spectrum of forces in large target condition.**

400 **A)** Average curve and standard deviation of influence of the Synch Participant's forces on the  
 401 Target Participant's ( $I_{S \rightarrow T}$ , red trace) and the Target Participant's forces on the Synch  
 402 Participant's ( $I_{T \rightarrow S}$ , blue trace). The average curve and standard deviation were estimated from  
 403 20 individuals (10 dyads x 2 directions). **B)** Overall differences between inter partner  
 404 influence ( $I_{S \rightarrow T} - I_{T \rightarrow S}$ ) are presented for the two frequency bands of [0-2.15] Hz and [2.15-7]  
 405 Hz;  $\Delta$  influence is the difference between each dyad participant's GGC's integral, estimated  
 406 in each frequency band of interest. Bars represent the mean difference; dots represent the  
 407 difference for each dyad. The Synch Participant's influence on the Target Participant ( $I_{S \rightarrow T}$ )  
 408 was similar to its counterpart in the [0-2.15] Hz frequency band ( $T(18)=1.22$ ,  $p=0.24$ , two-  
 409 sample t-test) but significantly higher in the [2.15-7] Hz frequency band ( $T(18)=5.88$ ,  
 410  $p<0.001$ , two-sample t-test).

411



412

413 **Fig. 6) Granger-Geweke causality (GGC) spectrum of forces in small target condition.**

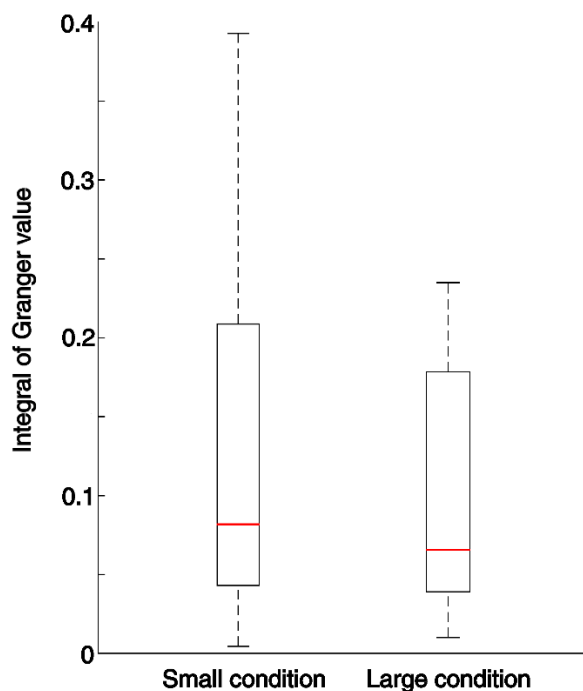
414 **A)** Average curve and standard deviation of influence of the Synch Participant's forces on the

415 Target Participant's ( $I_{S \rightarrow T}$ , red trace) and the Target Participant's forces on the Synch  
416 Participant's ( $I_{T \rightarrow S}$ , blue trace). The average curve and standard deviation were estimated from  
417 20 individuals (10 dyads x 2 directions). **B)** Overall differences between inter partner  
418 influence ( $I_{S \rightarrow T} - I_{T \rightarrow S}$ ) are presented for the two frequency bands of [0-2.15] Hz and [2.15-7]  
419 Hz. The Synch Participant's influence on the Target Participant ( $I_{S \rightarrow T}$ ) was similar to its  
420 counterpart in the [0-2.15] Hz frequency band ( $T(18)=1.10$ ,  $p>0.28$ , two-sample t-test) but  
421 significantly higher in the [2.15-7] Hz frequency band ( $T(18)=5.89$ ,  $p<0.001$ , two-sample t-  
422 test).

423

424 These results are similar to that obtained in our previous study. Even though changes  
425 were applied to the targets' width (i.e. in the Target Participant tasks), the Synch  
426 Participant remains the most influential in both conditions.

427 We also hypothesized that if the influence we measured using GGC analysis had a  
428 relation to information exchange, its quantity would increase with the difficulty of the  
429 task. To address this issue, we looked at the overall quantitative influence, measured  
430 in a dyad by the sum of partners' integral of GGC values over frequency, and  
431 compared it between conditions. We observed that the overall quantitative influence  
432 was significantly higher in the small target condition than in the large target condition  
433 ( $W=185$ ,  $p<0.003$ , Wilcoxon signed rank test, Fig. 7).



434

435 **Fig. 7) Comparison of influence between conditions.** Box plot of the total influence,  
436 estimated from the integral of GGC values of participants in a dyad across frequencies, for  
437 each condition. The total inter-personal influence was significantly less in the large target  
438 condition compared to the small target condition ( $W=185$ ,  $p<0.003$ , Wilcoxon signed rank  
439 test).

440 To better understand this result we analyzed the overall influence (on the partner) by  
441 each of the Target and Synch Participants, and over the two frequency bands, using a

442 Three-Way Mixed effect ANOVA. We found a significant main effect of target sizes  
443 on influence ( $F(1,18)=16.8$ ,  $p<0.001$ ), as well as frequency bands ( $F(1,18)=9.5$ ,  
444  $p<0.006$ ). A significant main effect of roles in influence scores was also observed  
445 ( $F(1,18)=15.6$ ,  $p<0.001$ ). The results also showed a significant interaction between  
446 frequency bands and roles in terms of influence ( $F(1,18)=6.8$ ,  $p<0.02$ ). No other  
447 significant interaction was found.

448 To investigate our interactions, we used a Bonferroni post-hoc test (see  
449 Supplementary figures for tables). We observed that Sync Participants had a  
450 significant higher influence on their partners in both small and large target conditions  
451 (Small,  $T(9)=4.3$ ,  $p<0.002$  ; Large,  $T(9)=3.2$ ,  $p<0.03$ ). Sync Participants were also  
452 found to significantly influence more their partners in the [2.15-7] Hz frequency band  
453 ( $T(9)=4.7$ ,  $p<0.001$ ) and this in both conditions (Small,  $T(9)=5.2$ ,  $p<0.001$  ; Large,  
454  $T(9)=3.6$ ,  $p<0.025$ ). No significant difference was found in the [0-2.15] Hz frequency  
455 band. Thus, the augmentation on the overall quantitative influence in the small target  
456 condition is overly due to an augmentation of the Synch Participant's influence.

457

458 Finally, we used a Pearson correlation to measure the correlation between the  
459 difference of integral of  $\Delta$  influence over frequency and the performance indices in  
460 both conditions. In the [0-2.15] Hz frequency band, we found a significant positive  
461 correlation between the  $\Delta$  influence and the Synchronization Error standard deviation  
462 (SEsd) in the large target condition ( $p<0.0013$ ,  $r=0.86$ ). We did not find any other  
463 significant correlation in any condition and in any frequency band.

464

#### 465 **4. Discussion**

466 Interactive forces are a key element in physical interaction, not only as an energy  
467 provider but also as a fundamental feature of successful inter-personal coordination  
468 (Takagi et al., 2018; Takagi et al., 2017; Melendez-Calderon et al., 2015). We were  
469 interested in understanding how these forces could help dyads to work together and  
470 exchange information through the haptic sense. For this we used a setup specially  
471 conceived so information exchange would be necessary to the completion of the task.  
472 By dividing the information accessible by each partner, attributing them the roles of  
473 Synch and Target Participants, we enforced the need for them to engage in the task at  
474 all times and cooperate. We chose this method over others, like modulating the noise  
475 in the feedbacks available to the partners (Takagi et al., 2018), or limiting their motor  
476 ability in the task (van der Wel et al., 2011), so as to ensure that none of the  
477 participants could complete the task alone and both felt compelled to participate.

478 The choice to have two conditions of different difficulty was made so we could  
479 observe the way our participants would adapt, with the hypothesis that a higher  
480 difficulty would result in a higher quantity of information exchanged. We have  
481 previously shown that the information exchange between dyad participants can be  
482 quantified by using Granger-Geweke causality (GGC) (Colomer et al., 2022). Here  
483 we applied the same technique to evaluate how the information exchange changes  
484 with task difficulty.

485 From the analysis of the interacting forces generated during the task using GGC, we  
486 found a significant higher influence from the Synch Participant over the Target  
487 Participant in the [2.15-7] Hz frequency band corroborating the findings from our  
488 previous experiment, under both conditions. The total influence (Fig. 7) increased in  
489 the small target condition when the difficulty of the task was increased by reaching to  
490 a smaller target. On the other hand, we found that the mean force by each participant  
491 was higher in the large target condition (Fig. 4A). This is not surprising given that it  
492 was the condition where movements were fastest, as predicted from Fitts law.

493 However it is interesting to highlight the fact that the change of total influence  
494 between conditions is due to an augmentation of the Synch Participant's influence on  
495 the Target Participant in the small target condition. We did not expect this result  
496 because the change of difficulty in our experiment occurred in the spatial dimension,  
497 that is, the Target Participant's task. We can however envision a possible explanation  
498 for this adaptation. As the width of the target decreases, so does the time spent in it. A  
499 finer control of the task is therefore required to ensure that the metronome beat will  
500 occur while the mobile slider is within the target. This control is performed by the  
501 Synch Participant, as the change in influence suggests. No change was observed in the  
502 magnitude of the force produced by the Synch Participant between conditions, but we  
503 found a significant difference in force's frequency content distributions between small  
504 and large target conditions for both Target and Synch Participants (Fig. 3B and 3C).  
505 Only the Target Participants' mean frequency content was correlated with the  
506 movement time period. Thus, we can argue that while the change in the frequency  
507 content in the Target Participants' forces was due to a change of time movement  
508 inherent to the task, the change in frequency content in the Synch Participants' forces  
509 relates to an increase of influence, through an increase of higher frequencies in their  
510 forces (Fig. 3C).

511 Granger causality represents the magnitude of causal influence (Geweke, 1982;  
512 Granger, 1969) between the partners in an interaction. In this study we expected and  
513 found results in line with our previous findings (Colomer et al., 2022). That is, a  
514 superior influence exerted by the Synch Participants' on the Targets Participants  
515 within the [2.15-7] Hz range. However, while we expected an increase in the GGC  
516 values in the more difficult condition using smaller targets (Fitts, 1954), we did not  
517 expect the influence to come from the Synch Participants. This pattern of cooperation  
518 was spontaneously and unanimously adopted by our dyads, within a short time  
519 adaptation window and without verbal or facial communication. A clear task division  
520 was observable between our participants. The Target Participant took up more of the  
521 effort input required for the task, inputting larger forces of lower frequency. The  
522 Synch Participant on the other hand, applied forces of higher frequency that  
523 influenced the Target Participant more than the other way around.

524 It is proposed that humans in physical interaction naturally assume different roles like  
525 'leader' and 'follower' (Jarrassé et al., 2014, Melendez-Calderon et al., 2015, Reed  
526 and Peshkin 2008, Ueha et al., 2009) and it could be argued that in our study the  
527 Synch Participants, whose forces contributed the most to the total information  
528 exchanges, were leaders. While this phenomenon is not yet fully understood, we  
529 believe role and task division studies are a necessary step to better understand

530 information exchange during haptic interaction (see Losey et al., 2018 for review) and  
531 that Granger-Geweke causality can be a useful tool in leadership estimation.

532

### 533 **Acknowledgments**

534 Authors thank Ding, Bressler Chen et al. for making the toolbox Bsmart publicly  
535 available. We also thank Simon Pla for building the experiment apparatus setup and  
536 Avik Hovhannissian for helping us during acquisitions.

537

538 **Funding:** This study was financially supported by the European Project  
539 ENTIMEMENT, H2020-FETPROACT-2018, Grant Number 824160.

540

541 **Competing interests:** Authors declare that they have no competing interests.

542

### 543 **References**

- 544 1. Bressler, S. L., & Seth, A. K. (2011). Wiener–Granger Causality : A well  
545 established methodology. *NeuroImage*, 58(2), 323-329.  
546 <https://doi.org/10.1016/j.neuroimage.2010.02.059>
- 547 2. Brovelli, A., Ding, M., Ledberg, A., Chen, Y., Nakamura, R., & Bressler, S. L.  
548 (2004). Beta oscillations in a large-scale sensorimotor cortical network :  
549 Directional influences revealed by Granger causality. *Proceedings of the*  
550 *National Academy of Sciences*, 101(26), 9849-9854.  
551 <https://doi.org/10.1073/pnas.0308538101>
- 552 3. Cascio, C. J., Moore, D., & McGlone, F. (2019). Social touch and human  
553 development. *Developmental Cognitive Neuroscience*, 35, 5-11.  
554 <https://doi.org/10.1016/j.dcn.2018.04.009>
- 555 4. Chackochan, V. T., & Sanguineti, V. (2019). Incomplete information about  
556 the partner affects the development of collaborative strategies in joint action.  
557 *PLoS Computational Biology*, 15(12).  
558 <https://doi.org/10.1371/journal.pcbi.1006385>
- 559 5. Colomer, C., Dhamala, M., Ganesh, G., & Lagarde, J. Interacting humans use  
560 forces in specific frequencies to exchange information by touch. (in press),  
561 *Scientific Reports*. Preprint available: [https://hal.archives-ouvertes.fr/hal-](https://hal.archives-ouvertes.fr/hal-03763684)  
562 [03763684](https://hal.archives-ouvertes.fr/hal-03763684)
- 563 6. Cui, J., Xu, L., Bressler, S. L., Ding, M., & Liang, H. (2008). BSMART : A  
564 Matlab/C toolbox for analysis of multichannel neural time series. *Neural*  
565 *Networks: The Official Journal of the International Neural Network Society*,  
566 21(8), 1094-1104. <https://doi.org/10.1016/j.neunet.2008.05.007>
- 567 7. Craig, C., Pepping, G. J., & Grealy, M. (2005). Intercepting beats in  
568 predesignated target zones. *Experimental brain research*, 165(4), 490-504.
- 569 8. Curioni, A., Vesper, C., Knoblich, G., & Sebanz, N. (2019). Reciprocal  
570 information flow and role distribution support joint action coordination.  
571 *Cognition*, 187, 21-31. <https://doi.org/10.1016/j.cognition.2019.02.006>
- 572 9. De Leva, P. (1996). ADJUSTMENTS TO ZATSIORSKY-SELUYANOV" S  
573 SEGMENT IN ERTIA PARAMETERS. *J biomech*, 29(9), 1223-1230.

- 574 10. Dhamala, M., Liang, H., Bressler, S. L., & Ding, M. (2018). Granger-Geweke  
575 causality : Estimation and interpretation. *NeuroImage*, 175, 460-463.  
576 <https://doi.org/10.1016/j.neuroimage.2018.04.043>
- 577 11. Dhamala, M., Rangarajan, G., & Ding, M. (2008). Estimating Granger  
578 Causality from Fourier and Wavelet Transforms of Time Series Data. *Physical*  
579 *Review Letters*, 100(1), 018701.  
580 <https://doi.org/10.1103/PhysRevLett.100.018701>
- 581 12. Ding, M., Chen, Y., & Bressler, S. L. (2006). Granger Causality : Basic  
582 Theory and Application to Neuroscience. *ArXiv:Q-Bio/0608035*.  
583 <http://arxiv.org/abs/q-bio/0608035>
- 584 13. Dowd, C. (2020). A New ECDF Two-Sample Test Statistic.  
585 *ArXiv:2007.01360 [Stat]*. <http://arxiv.org/abs/2007.01360>
- 586 14. Fitts, P. M. (1954). The information capacity of the human motor system in  
587 controlling the amplitude of movement. *Journal of Experimental Psychology*,  
588 47(6), 381-391. <https://doi.org/10.1037/h0055392>
- 589 15. Fumery, G., Turpin, N. A., Claverie, L., Fourcassié, V., & Moretto, P. (2021).  
590 A biomechanical study of load carriage by two paired subjects in response to  
591 increased load mass. *Scientific Reports*, 11(1), 4346.  
592 <https://doi.org/10.1038/s41598-021-83760-6>
- 593 16. Gallace, A., & Spence, C. (2010). The science of interpersonal touch: An  
594 overview. *Neuroscience & Biobehavioral Reviews*, 34(2), 246-259.  
595 <https://doi.org/10.1016/j.neubiorev.2008.10.004>
- 596 17. Ganesh, G., Takagi, A., Osu, R., Yoshioka, T., Kawato, M., & Burdet, E.  
597 (2014). Two is better than one: Physical interactions improve motor  
598 performance in humans. *Scientific Reports*, 4, 3824.  
599 <https://doi.org/10.1038/srep03824>
- 600 18. Geweke, J. (1982). Measurement of Linear Dependence and Feedback  
601 between Multiple Time Series. *Journal of the American Statistical*  
602 *Association*, 77(378), 304-313.  
603 <https://doi.org/10.1080/01621459.1982.10477803>
- 604 19. Granger, C. W. J. (1969). *Investigating Causal Relations by Econometric*  
605 *Models and Cross-spectral Methods*. 16.
- 606 20. Huys, R., Kolodziej, A., Lagarde, J., Farrer, C., Darmana, R., & Zanone, P. G.  
607 (2018). Individual and dyadic rope turning as a window into social  
608 coordination. *Human Movement Science*, 58, 55-68.
- 609 21. Jarrassé, N., Sanguineti, V., & Burdet, E. (2014). Slaves no longer: Review on  
610 role assignment for human-robot joint motor action. *Adaptive Behavior*, 22(1),  
611 70-82. <https://doi.org/10.1177/1059712313481044>
- 612 22. Jerbi, K., Lachaux, J.-P., N'Diaye, K., Pantazis, D., Leahy, R. M., Garnero, L.,  
613 & Baillet, S. (2007). Coherent neural representation of hand speed in humans  
614 revealed by MEG imaging. *Proceedings of the National Academy of Sciences*,  
615 104(18), 7676-7681. <https://doi.org/10.1073/pnas.0609632104>
- 616 23. Kelso, J. A. S. (1995). *Dynamic Patterns: The Self-organization of Brain and*  
617 *Behavior*. MIT Press.
- 618 24. Knoblich, G., & Jordan, J. S. (2003). Action coordination in groups and  
619 individuals: Learning anticipatory control. *Journal of Experimental*  
620 *Psychology: Learning, Memory, and Cognition*, 29(5), 1006-1016.  
621 <https://doi.org/10.1037/0278-7393.29.5.1006>

- 622 25. Lederman, S. J., & Klatzky, R. L. (2009). Haptic perception : A tutorial.  
623 *Attention, Perception & Psychophysics*, 71(7), 1439-1459.  
624 <https://doi.org/10.3758/APP.71.7.1439>
- 625 26. Losey, D. P., McDonald, C. G., Battaglia, E., & O'Malley, M. K. (2018). A  
626 Review of Intent Detection, Arbitration, and Communication Aspects of  
627 Shared Control for Physical Human–Robot Interaction. *Applied Mechanics*  
628 *Reviews*, 70(1). <https://doi.org/10.1115/1.4039145>
- 629 27. Melendez-Calderon, A., Komisar, V., & Burdet, E. (2015). Interpersonal  
630 strategies for disturbance attenuation during a rhythmic joint motor action.  
631 *Physiology & Behavior*, 147, 348-358.  
632 <https://doi.org/10.1016/j.physbeh.2015.04.046>
- 633 28. Miall, R. C., Weir, D. J., & Stein, J. F. (1993). Intermittency in Human  
634 Manual Tracking Tasks. *Journal of Motor Behavior*, 25(1), 53-63.  
635 <https://doi.org/10.1080/00222895.1993.9941639>
- 636 29. Noy, L., Dekel, E., & Alon, U. (2011). The mirror game as a paradigm for  
637 studying the dynamics of two people improvising motion together.  
638 *Proceedings of the National Academy of Sciences*, 108(52), 20947-20952.  
639 <https://doi.org/10.1073/pnas.1108155108>
- 640 30. Ramdas, A., Trillos, N. G., & Cuturi, M. (2017). On Wasserstein Two-Sample  
641 Testing and Related Families of Nonparametric Tests. *Entropy*, 19(2), 47.  
642 <https://doi.org/10.3390/e19020047>
- 643 31. Reed, K. B., & Peshkin, M. A. (2008). Physical Collaboration of Human-  
644 Human and Human-Robot Teams. *IEEE Transactions on Haptics*, 1(2),  
645 108-120. <https://doi.org/10.1109/TOH.2008.13>
- 646 32. Sabu, S., Curioni, A., Vesper, C., Sebanz, N., & Knoblich, G. (2020). How  
647 does a partner's motor variability affect joint action? *PLOS ONE*, 15(10),  
648 e0241417. <https://doi.org/10.1371/journal.pone.0241417>
- 649 33. Sailer, U., & Leknes, S. (2022). Meaning makes touch affective. *Current*  
650 *Opinion in Behavioral Sciences*, 44, 101099.  
651 <https://doi.org/10.1016/j.cobeha.2021.101099>
- 652 34. Sawers, A., Bhattacharjee, T., McKay, J. L., Hackney, M. E., Kemp, C. C., &  
653 Ting, L. H. (2017). Small forces that differ with prior motor experience can  
654 communicate movement goals during human-human physical interaction.  
655 *Journal of NeuroEngineering and Rehabilitation*, 14(1), 8.  
656 <https://doi.org/10.1186/s12984-017-0217-2>
- 657 35. Sebanz, N., & Knoblich, G. (2009). Prediction in Joint Action : What, When,  
658 and Where. *Topics in Cognitive Science*, 1(2), 353-367.  
659 <https://doi.org/10.1111/j.1756-8765.2009.01024.x>
- 660 36. Shannon, C. E. (1948). A mathematical theory of communication. *The Bell*  
661 *System Technical Journal*, 27(3), 379-423. [https://doi.org/10.1002/j.1538-](https://doi.org/10.1002/j.1538-7305.1948.tb01338.x)  
662 [7305.1948.tb01338.x](https://doi.org/10.1002/j.1538-7305.1948.tb01338.x)
- 663 37. Sylos-Labini, F., d'Avella, A., Lacquaniti, F., & Ivanenko, Y. (2018). Human-  
664 Human Interaction Forces and Interlimb Coordination During Side-by-Side  
665 Walking With Hand Contact. *Frontiers in Physiology*, 9.  
666 <https://doi.org/10.3389/fphys.2018.00179>
- 667 38. Takagi, A., Ganesh, G., Yoshioka, T., Kawato, M., & Burdet, E. (2017).  
668 Physically interacting individuals estimate the partner's goal to enhance their  
669 movements. *Nature Human Behaviour*, 1(3), 0054.  
670 <https://doi.org/10.1038/s41562-017-0054>

- 671       **39.** Takagi, A., Usai, F., Ganesh, G., Sanguineti, V., & Burdet, E. (2018). Haptic  
672       communication between humans is tuned by the hard or soft mechanics of  
673       interaction. *PLOS Computational Biology*, *14*(3), e1005971.  
674       <https://doi.org/10.1371/journal.pcbi.1005971>
- 675       **40.** Tomassini, A., Laroche, J., Emanuele, M., Nazzaro, G., Petrone, N., Fadiga,  
676       L., & D'Ausilio, A. (2022). Interpersonal synchronization of movement  
677       intermittency. *IScience*, *25*(4), 104096.  
678       <https://doi.org/10.1016/j.isci.2022.104096>
- 679       **41.** Ueha, R., Pham, H. T. T., Hirai, H., & Miyazaki, F. (2009). Dynamical role  
680       division between two subjects in a crank-rotation task. *2009 IEEE*  
681       *International Conference on Rehabilitation Robotics*, 701-706.  
682       <https://doi.org/10.1109/ICORR.2009.5209584>
- 683       **42.** van der Wel, R. P. R. D., Knoblich, G., & Sebanz, N. (2011). Let the force be  
684       with us: Dyads exploit haptic coupling for coordination. *Journal of*  
685       *Experimental Psychology: Human Perception and Performance*, *37*(5),  
686       1420-1431. <https://doi.org/10.1037/a0022337>
- 687       **43.** Woodworth, R. S. (1899). Accuracy of voluntary movement. *The*  
688       *Psychological Review: Monograph Supplements*, *3*(3), i-114.  
689       <https://doi.org/10.1037/h0092992>

